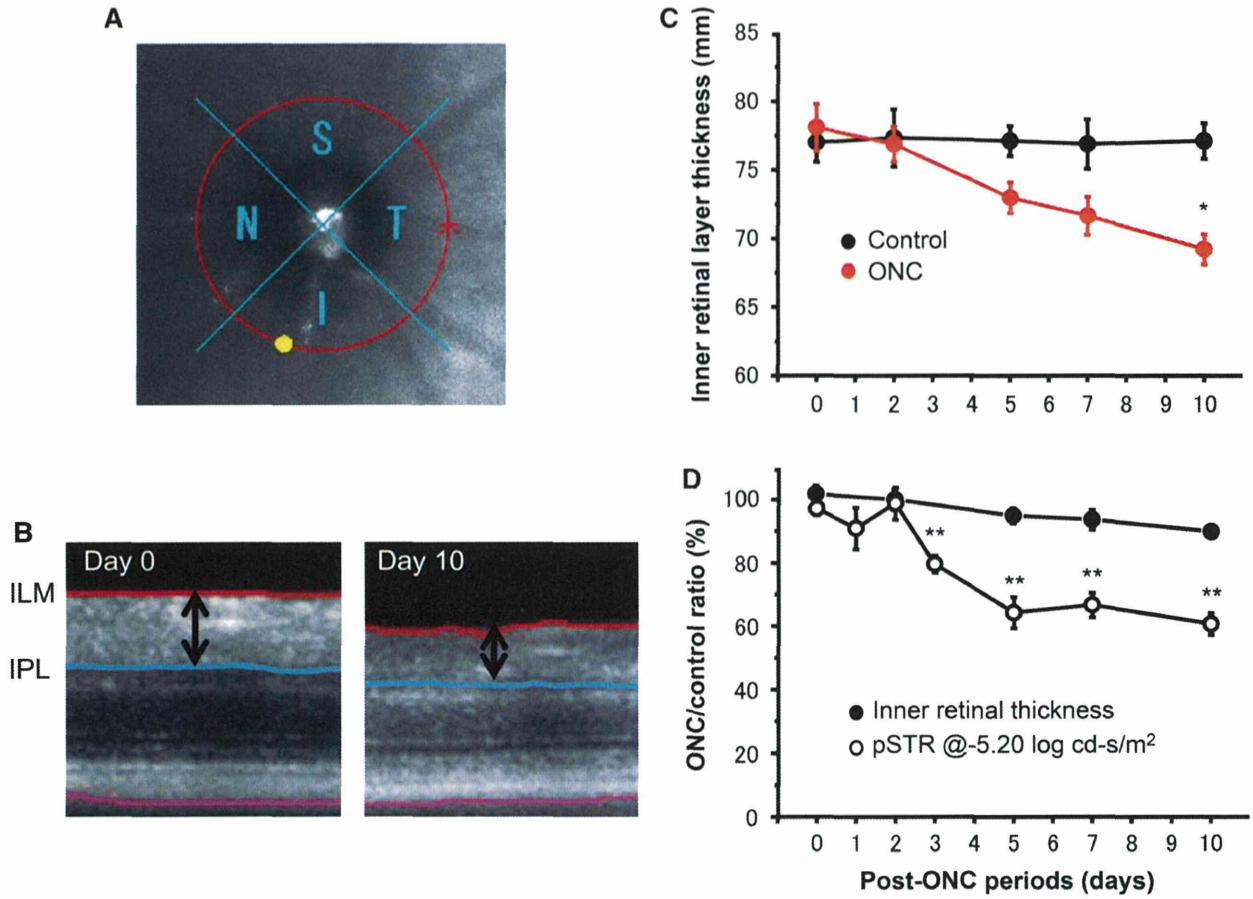

Fig. 4 SD-OCT images were acquired circumferentially around the optic nerve head (**a**). Representative SD-OCT images obtained from the same eye before (day 0, *left*) and after ONC (day 10, *right*) (**b**). The distance between the internal limiting membrane and inner plexiform layer was measured in order to determine the inner retinal thickness (indicated by the *arrow* in **b**). The inner retinal thickness was plotted against the post-ONC time course for the control and ONC eyes (**c**, $I = 9$ for each time point). The pSTR amplitude and inner retinal thickness of the ONC eyes were normalized to those of the contralateral control eyes, expressed as a percentage and plotted as a function of the post-ONC time course (**d**). *SD-OCT* spectral-domain optical coherence tomography, *ONC* optic nerve crush, *S* superior, *T* temporal, *I* inferior, *N* nasal, *ILM* internal limiting membrane, *IPL* inner plexiform layer, *pSTR* positive scotopic threshold response, *error bars* standard error, $^*P < 0.01$

patients with traumatic optic neuropathy, the PhNR, which reflects RGC function, deteriorates before there is significant loss of retinal nerve fiber layer thickness [10]. Taken together, these findings therefore suggest that functional alterations in the RGCs precede the anatomical loss of the RGCs themselves.

We also observed the expression of genes that determine specific RGC types [24, 25] as early as day 1. This molecular alteration preceded the functional and morphological changes detected by the pSTR or SD-OCT, indicating that changes at the molecular level have begun, while RGCs are still preserved and functioning.

A recent study of the changes induced by ONC found that pSTR began to decrease on day 7 [26], in contrast to our finding that a reduction had already occurred on day 3. This discrepancy may be due to a number of possible factors. First, we performed ONC by crushing the optic nerve with forceps for 5 s, while Lui et al. crushed the optic nerve for only 4 s. This difference could explain the earlier manifestation of the loss of RGC function in our study. Second, we normalized the pSTR amplitude to the value of the contralateral untreated eye, in order to reduce the influence of inter-animal variation and improve the sensitivity of our experiment. Therefore, we believe

that the sensitivity of our measurements was relatively high, lending credence to our findings.

One of the previously noted limitations of measuring RGC function with the ERG is that RGC function depends on inputs from upstream neurons such as photoreceptors and bipolar cells [16]. However, we found that the a- and b-waves, which depend on the function of the photoreceptors and bipolar cells, remained unchanged after ONC throughout the experiment, indicating that ONC did not affect the function of these upstream neurons. This suggests that alterations in the pSTR reflect abnormal function of the RGCs.

RGC function can also be evaluated by measuring pattern ERG in mice [27]. However, it has not been determined how early after ONC, the pattern ERG begins to deteriorate in mice. Measuring the visual evoked potential (VEP) is another method of evaluating RGC function. However, ONC immediately suppresses the VEP, even while RGCs continue to survive for some time. Therefore, measurements of the VEP cannot serve as markers of RGC function in experiments using ONC. In conclusion, we confirmed that changes in the pSTR reflected early losses of RGC function after ONC, raising the possibility that the pSTR could be used in monitoring the effects of novel therapies to protect RGCs in the early stages of degeneration. Furthermore, changes in RGC-specific gene expression preceded anatomical and functional changes in the RGCs themselves.

Acknowledgments We thank Ms. Junko Sato for her technical assistance. This work was supported in part by JSPS KAKENHI Grants-in-Aid for Scientific Research B (T.N. 26293372) and for Challenging Exploratory Research (Y.T. 26670263 and T.N. 26670751). This study was also supported by the JST Center for Revitalization Promotion (Y.T. and T.N.).

Conflict of interest The authors have no conflict of interest.

References

1. Heijl A, Leske MC, Bengtsson B, Hyman L, Bengtsson B, Hussein M, Early Manifest Glaucoma Trial G (2002) Reduction of intraocular pressure and glaucoma progression: results from the Early Manifest Glaucoma Trial. Arch Ophthalmol 120(10):1268–1279
2. Collaborative Normal-Tension Glaucoma Study Group (1998) The effectiveness of intraocular pressure reduction in the treatment of normal-tension glaucoma. Am J Ophthalmol 126(4):498–505
3. Musch DC, Gillespie BW, Lichter PR, Niziol LM, Janz NK, Investigators CS (2009) Visual field progression in the Collaborative Initial Glaucoma Treatment Study the impact of treatment and other baseline factors. Ophthalmology 116(2):200–207. doi:10.1016/j.ophtha.2008.08.051
4. Ryu M, Yasuda M, Shi D, Shanab AY, Watanabe R, Himori N, Omodaka K, Yokoyama Y, Takano J, Saido T, Nakazawa T (2012) Critical role of calpain in axonal damage-induced retinal ganglion cell death. J Neurosci Res 90(4):802–815. doi:10.1002/jnr.22800
5. Himori N, Yamamoto K, Maruyama K, Ryu M, Taguchi K, Yamamoto M, Nakazawa T (2013) Critical role of Nrf2 in oxidative stress-induced retinal ganglion cell death. J Neurochem 127(5):669–680. doi:10.1111/jnc.12325
6. Fujita Y, Sato A, Yamashita T (2013) Brimonidine promotes axon growth after optic nerve injury through Erk phosphorylation. Cell Death Dis 4:e763. doi:10.1038/cddis.2013.298
7. Yasuda M, Tanaka Y, Ryu M, Tsuda S, Nakazawa T (2014) RNA sequence reveals mouse retinal transcriptome changes early after axonal injury. PLoS One 9(3):e93258. doi:10.1371/journal.pone.0093258
8. Viswanathan S, Frishman LJ, Robson JG, Harwerth RS, Smith EL 3rd (1999) The photopic negative response of the macaque electroretinogram: reduction by experimental glaucoma. Invest Ophthalmol Vis Sci 40(6):1124–1136
9. Viswanathan S, Frishman LJ, Robson JG, Walters JW (2001) The photopic negative response of the flash electroretinogram in primary open angle glaucoma. Invest Ophthalmol Vis Sci 42(2):514–522
10. Gotoh Y, Machida S, Tazawa Y (2004) Selective loss of the photopic negative response in patients with optic nerve atrophy. Arch Ophthalmol 122(3):341–346. doi:10.1001/archopht.122.3.341
11. Rangaswamy NV, Frishman LJ, Dorotheo EU, Schiffman JS, Bahrani HM, Tang RA (2004) Photopic ERGs in patients with optic neuropathies: comparison with primate ERGs after pharmacologic blockade of inner retina. Invest Ophthalmol Vis Sci 45(10):3827–3837. doi:10.1167/iovs.04-0458
12. Miyata K, Nakamura M, Kondo M, Lin J, Ueno S, Miyake Y, Terasaki H (2007) Reduction of oscillatory potentials and photopic negative response in patients with autosomal dominant optic atrophy with OPA1 mutations. Invest Ophthalmol Vis Sci 48(2):820–824. doi:10.1167/iovs.06-0845
13. Machida S, Gotoh Y, Toba Y, Ohtaki A, Kaneko M, Kurosaka D (2008) Correlation between photopic negative response and retinal nerve fiber layer thickness and optic disc topography in glaucomatous eyes. Invest Ophthalmol Vis Sci 49(5):2201–2207. doi:10.1167/iovs.07-0887
14. Wang J, Cheng H, Hu YS, Tang RA, Frishman LJ (2012) The photopic negative response of the flash electroretinogram in multiple sclerosis. Invest Ophthalmol Vis Sci 53(3):1315–1323. doi:10.1167/iovs.11-8461
15. Machida S, Raz-Prag D, Fariss RN, Sieving PA, Bush RA (2008) Photopic ERG negative response from amacrine cell signaling in RCS rat retinal degeneration. Invest Ophthalmol Vis Sci 49(1):442–452. doi:10.1167/iovs.07-0291
16. Bui BV, Fortune B (2004) Ganglion cell contributions to the rat full-field electroretinogram. J Physiol 555(Pt 1):153–173. doi:10.1113/jphysiol.2003.052738

17. Sieving PA, Frishman LJ, Steinberg RH (1986) Scotopic threshold response of proximal retina in cat. J Neurophysiol 56(4):1049–1061
18. Frishman LJ, Shen FF, Du L, Robson JG, Harwerth RS, Smith EL 3rd, Carter-Dawson L, Crawford ML (1996) The scotopic electroretinogram of macaque after retinal ganglion cell loss from experimental glaucoma. Invest Ophthalmol Vis Sci 37(1):125–141
19. Mojumder DK, Sherry DM, Frishman LJ (2008) Contribution of voltage-gated sodium channels to the b-wave of the mammalian flash electroretinogram. J physiol 586(10):2551–2580. doi:10.1113/jphysiol.2008.150755
20. Smith BJ, Wang X, Chauhan BC, Cote PD, Tremblay F (2014) Contribution of retinal ganglion cells to the mouse electroretinogram. Doc Ophthalmol Adv Ophthalmol. doi:10.1007/s10633-014-9433-2
21. Shanab AY, Nakazawa T, Ryu M, Tanaka Y, Himori N, Taguchi K, Yasuda M, Watanabe R, Takano J, Saido T, Minegishi N, Miyata T, Abe T, Yamamoto M (2012) Metabolic stress response implicated in diabetic retinopathy: the role of calpain, and the therapeutic impact of calpain inhibitor. Neurobiol Dis 48(3):556–567. doi:10.1016/j.nbd.2012.07.025
22. Alarcon-Martinez L, Aviles-Trigueros M, Galindo-Romero C, Valiente-Soriano J, Agudo-Barriuso M, Villa Pde L, Villegas-Perez MP, Vidal-Sanz M (2010) ERG changes in albino and pigmented mice after optic nerve transection. Vision Res 50(21):2176–2187. doi:10.1016/j.visres.2010.08.014
23. Kohzaki K, Vingrys AJ, Bui BV (2008) Early inner retinal dysfunction in streptozotocin-induced diabetic rats. Invest Ophthalmol Vis Sci 49(8):3595–3604. doi:10.1167/iovs.08-1679
24. Shi M, Kumar SR, Motajo O, Kretschmer F, Mu X, Badea TC (2013) Genetic interactions between Brn3 transcription factors in retinal ganglion cell type specification. PLoS One 8(10):e76347. doi:10.1371/journal.pone.0076347
25. Sajgo S, Ghinia MG, Shi M, Liu P, Dong L, Parmhans N, Popescu O, Badea TC (2014) Dre-cre sequential recombination provides new tools for retinal ganglion cell labeling and manipulation in mice. PLoS One 9(3):e91435. doi:10.1371/journal.pone.0091435
26. Liu Y, McDowell CM, Zhang Z, Tebow HE, Wordinger RJ, Clark AF (2014) Monitoring retinal morphologic and functional changes in mice following optic nerve crush. Invest Ophthalmol Vis Sci 55(6):3766–3774. doi:10.1167/iovs.14-13895
27. Porciatti V (2007) The mouse pattern electroretinogram. Doc Ophthalmol Adv Ophthalmol 115(3):145–153. doi:10.1007/s10633-007-9059-8

nata (as required), which did not affect the risk of having a case of post-intravitreal injection endophthalmitis ($P = 0.503$). In the multivariate analysis, no potentially modifiable risk factors were identified to increase post-intravitreal injection endophthalmitis.

This survey sought to establish some of the practices of Victorian ophthalmologists who perform intravitreal injections to treat neovascular AMD, mainly in their private rooms. Although no potentially modifiable risk factors are identified for post-intravitreal injection endophthalmitis, some trends are shown. Of particular interest are the trends for those who see more patients and those who do not use a drape, and while these two factors are not linked, it is not possible to hypothesize whether 'time' is a factor. Major limitations of this study include the potential low number of responses, volunteer bias with an under-participation of those who may have had endophthalmitis and the retrospective design.

The authors are pleased to report that current practices in Victoria are consistent with current evidence. We thank all those who participated and believe that the information from this survey explores and helps ophthalmologists to keep thinking about potentially modifiable risk factors for optimal management in the prevention of post-intravitreal injection endophthalmitis.

Danielle A Buck MBBS BSc,[1]
Rosie Dawkins MBBS MPH,[1]
Ryo Kawasaki MD PhD,[2,3]
Sukhpal S Sandhu MD FRANZCO[1,3,4]
and **Penelope J Allen** FRANZCO[1,3,4]
[1]*Royal Victorian Eye and Ear Hospital,* [3]*Centre for Eye Research Australia, and* [4]*University of Melbourne, Melbourne, Victoria, Australia; and* [2]*Yamagata University Faculty of Medicine, Yamagata, Japan*
Received 15 March 2014; accepted 30 July 2014.

References

1. Harvey KJ, Day RO, Campbell WG *et al.* Saving money on the PBS: ranibizumab or bevacizumab for neovascular macular degeneration? *Med J Aust* 2011; **194**: 567–8.
2. Chen E, Lin MY, Cox J *et al.* Endophthalmitis after intravitreal injection: the importance of viridans streptococci. *Retina* 2011; **31**: 1525–33.
3. Lyall DA, Tey A, Foot B *et al.* Post-intravitreal anti-VEGF endophthalmitis in the United Kingdom: incidence, features, risk factors, and outcomes. *Eye* 2012; **26**: 1517–26.
4. McCannel CA. Meta-analysis of endophthalmitis after intravitreal injection of anti-vascular endothelial growth factor agents: causative organisms and possible prevention strategies. *Retina* 2011; **31**: 654–61.
5. Shah CP, Garg SJ, Vander JF *et al.* Outcomes and risk factors associated with endophthalmitis after intravitreal injection of anti-vascular endothelial growth factor agents. *Ophthalmology* 2011; **118**: 2028–34.

Regional correlation of macular areas and visual acuity in patients with open-angle glaucoma

Good vision is closely associated with quality of life (QOL). Visual function in eyes with retinal disease has two important parameters: the visual field (VF) and visual acuity (VA). Generally, QOL-affecting VF loss is a common symptom in glaucoma patients, and can lead to driving license revocation and reduced reading speed.[1] QOL can also be significantly disturbed by decreased VA. Recent studies have revealed that macular lesions are common in open-angle glaucoma (OAG).[2] However, there is currently only a limited understanding of the regional correlation of VA in the macular function. A greater understanding of these regional correlations would help diagnose the cause of decreased VA in patients and therefore be of significant clinical value. The purpose of this investigation was thus to determine the regional correlation of VA to sensitivity in the test points of the Humphrey field analyser 10-2 programme (HFA 10-2) or to optical coherence tomography (OCT) macular maps in patients with OAG.

This study included 60 eyes with OAG. The inclusion criteria were: OAG with a glaucomatous VF according to the Anderson-Patella classification and spherical equivalent (SE) refractive error of ≥8.00 D (i.e. excluding high myopia). The exclusion criteria were: decimal VA <0.3 and the presence of VF-affecting ocular or systemic diseases other than OAG. Best-corrected VA was measured with a standard Japanese decimal VA chart and converted to the logarithm of the minimum angle of resolution (logMAR) for statistical analysis. To assess macular function, HFA 10-2 threshold values, total deviation (TD) and pattern deviation (PD) were examined in reliably measured VFs (excluding measurements with <20% fixation errors and <33% false-positive or false-negative results). OCT (3D OCT-2000; TOPCON Corporation, Topcon Corporation, Tokyo, Japan) was used to measure the retinal nerve fibre layer (RNFL), ganglion cell complex (GCC) and ganglion cell layer plus inner plexiform layer (GCL + IPL) of the maps based on macular cube scans of a 6 × 6 mm square area centered on the fovea. Scans with image quality less than 70 or with inaccurate segmentation were excluded. All the examinations were performed within 3 months. Spearman's rank correlation coefficient was used to analyse the correlation between logMAR and each of the 68 HFA 10-2 test points, as well as the

Competing/conflicts of interest: No stated conflict of interest.

Funding sources: This paper was supported in part by a JST grant from JSPS KAKENHI Grants-in-Aid for Scientific Research (B) (T.N. 26293372) and for Exploratory Research (T.N. 26670751), and by JST Center for Revitalization Promotion.

This retrospective study was approved by the institutional review board of Tohoku University Graduate School of Medicine (study 2012-1-574).

This paper was presented at the Association of Research Visual Science 2013.

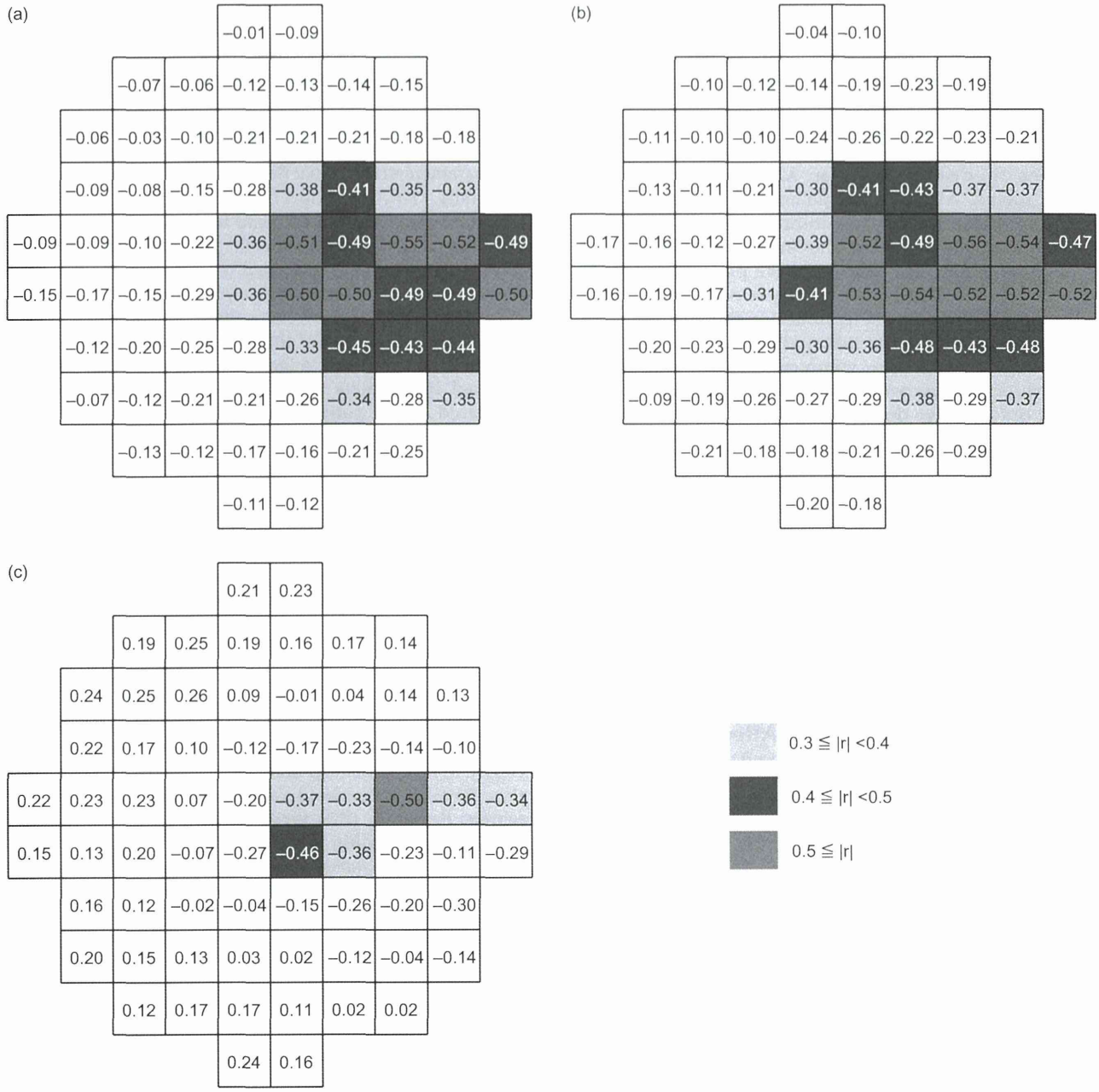

Figure 1. Distribution of Humphrey field analyser 10-2 programme (HFA 10-2) tests points correlated with visual acuity (VA). The grey-scale maps show the correlation coefficient of VA and HFA 10-2 measurements of threshold (a), total deviation (b) and pattern deviation (c). The right side of the figure represents the temporal visual field (the disc side) and the left side represents the nasal visual field. Darker shades of grey indicate a higher correlation coefficient, with a step scale of 0.1. Test points shown in white had no statistically significant correlation.

correlation between logMAR and each point on a 10×10 grid overlaid on the OCT macular maps.

Average demographic data for the patients in this study were as follows: age was 65.7 ± 11.1 years, SE was -2.8 ± 2.2 D, logMAR was 0.08 ± 0.28, HFA 30-2 mean deviation was -12.1 ± 8.9 dB, baseline intraocular pressure was 13.0 ± 3.2 mmHg and circumpapillary retinal nerve fibre layer thickness (cpRNFLT) was 79.3 ± 14.8 μm. Figure 1 shows the distribution of significantly VA-correlated HFA 10-2 test points. Test points with significantly VA-correlated threshold values ($r = -0.36$ to -0.55), TD ($r = -0.39$ to -0.56) and PD ($r = -0.33$ to -0.50) were mainly located in the area of the papillomacular bundle (PMB). Figure 2 shows the distribution of significantly VA-correlated grid points in the OCT macular maps. In the RNFL and GCC maps, the correlation coefficient with VA ranged from −0.30 to −0.54 and from −0.30 to −0.50, respectively. In these maps, the areas of significantly

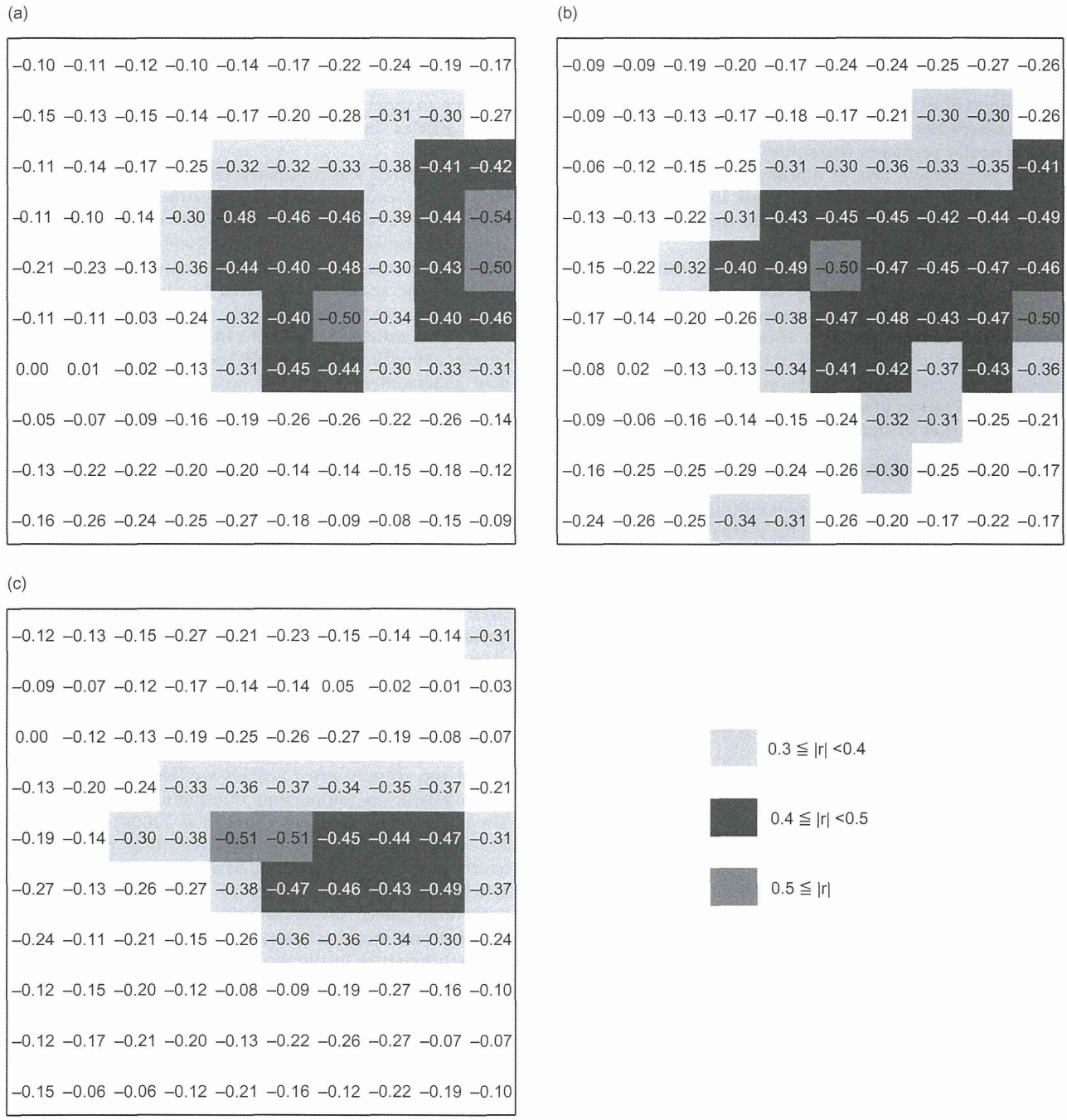

Figure 2. Distribution of optical coherence tomography (OCT) macular map grid points correlated with visual acuity (VA). The greyscale maps show the correlation coefficient of VA and the thickness of the retinal nerve fibre layer (RNFL) (a), ganglion cell complex (GCC) (b), and ganglion cell layer plus inner plexiform layer (GCL + IPL) (c). The right side of the figure represents the nasal (the disc side) and the left side represents the temporal. Darker shades of grey indicate a higher correlation coefficient, with a step scale of 0.1. Grid points shown in white had no statistically significant correlation.

correlated grid points were round and centered in the upper nasal region, which includes the PMB. In the GCL + IPL map, the correlation coefficient with VA ranged from −0.31 to −0.51. The correlated area in this map was flatter and closer to the PMB.

In the current study, we obtained data on the regional correlation of HFA 10-2 test points and the OCT macular map to VA in OAG patients. We found that areas with higher correlation ($r > 0.4$) were mainly located in the PMB. In a previous study, we demonstrated that cpRNFLT

in the temporal region, which includes the PMB, was significantly correlated to VA (r = −0.4) in patients with OAG.[3] We also found that the pathogenesis of this decreased VA may be related to myopia and decreased tissue blood flow in the temporal optic disc.[3] Interestingly, other research has found that patients with strong fluctuations in ocular perfusion pressure (OPP) also undergo significant progressive loss of macular function.[4] Decreased macular function is thus implicated in glaucoma, and decreased OPP may also be related to the pathogenesis of central VF deterioration.

In conclusion, we found that in patients with glaucoma, VA was strongly correlated to HFA 10-2 and the OCT macular map in the PMB area, suggesting that the analysis of regional data from the HFA 10-2 or OCT macular map may be a useful diagnostic tool in glaucoma patients with decreased VA. These findings also suggest that the involvement of the PMB in glaucomatous damage may make it a useful biomarker of significantly deteriorated QOL.

Acknowledgements

The authors thank Mr Tim Hilts for editing this manuscript and Dr Masahiro Akiba for useful discussion.

Kazuko Omodaka MD,[1] Takeshi Yabana MD,[1] Naoko Takada MD[1] and Toru Nakazawa MD PhD[1,2,3]

Departments of [1]Ophthalmology, [2]Retinal Disease Control and [3]Advanced Ophthalmic Medicine, Tohoku University Graduate School of Medicine, Sendai, Japan

Received 7 July 2014; accepted 15 July 2014.

References

1. Murata H, Hirasawa H, Aoyama Y *et al.* Identifying areas of the visual field important for quality of life in patients with glaucoma. *PLoS ONE* 2013; **8**: e58695.
2. Hood DC, Raza AS, de Moraes CG, Liebmann JM, Ritch R. Glaucomatous damage of the macula. *Prog Retin Eye Res* 2013; **32**: 1–21.
3. Omodaka K, Nakazawa T, Yokoyama Y, Doi H, Fuse N, Nishida K. Correlation between peripapillary macular fiber layer thickness and visual acuity in patients with open-angle glaucoma. *Clin Ophthalmol* 2010; **4**: 629–35.
4. Choi J, Lee JR, Lee Y *et al.* Relationship between 24-hour mean ocular perfusion pressure fluctuation and rate of paracentral visual field progression in normal-tension glaucoma. *Invest Ophthalmol Vis Sci* 2013; **54**: 6150–57.

Citation analysis of the most- and least-cited articles in *Clinical and Experimental Ophthalmology*: 2000–2013

Citation analysis has become a key tool used to judge and quantify the impact of scientific literature.[1,2] The fundamental measure is the journal citation count that assesses the frequency with which a published article is cited in the scientific literature.[1] To ascertain whether differences between most-cited and least-cited articles can be identified, we analysed the characteristics of the most- and least-cited articles in *Clinical and Experimental Ophthalmology* (*CEO*).

A core search was conducted (26 February 2014) via the Web of Science database (http://thomsonreuters.com/thomson-reuters-web-of-science/) for *'Clinical and Experimental Ophthalmology'* publications 2000–2013 (the journal was launched in 2000). To avoid inclusion of extraneous material, the search was refined by the primary journal document types 'Article', 'Letter', 'Editorial' and 'Review'. From 2355 articles identified (1434 original articles, 555 letters, 260 editorials and 106 reviews), a citation report was generated and ordered according to total citations received.

The 100 most-cited and 100 least-cited articles were analysed in terms of title, authors, year published, country, keywords, subject category, total citations and average citations per year. For simplicity, the corresponding author's institution determined country of origin. Subject categories were allocated according to the core theme and selected keywords, including: anterior segment, glaucoma, neuro-ophthalmology, visual sciences, uveitis, medical retinal, vitreoretinal, ocular genetics, ocular oncology, ophthalmic pharmacotherapy, oculoplastics and humanities. The 100 most-cited articles were determined by the number of total citations accrued. The 100 least-cited articles were identified from those that received zero citation in chronological order starting from year 2000.

The top 20 most-cited articles are listed in Table 1 (top 100 available as Supporting information – online only). The most-cited article, by Young *et al.* (2000) had accrued 233 citations.[3] Research groups featuring most prominently in the top 100 most-cited articles included those of Mitchell (Sydney) and McGhee (Auckland) – affiliated with eight and seven articles, respectively. Anterior segment and visual science topics were the most popular subject categories in the top 100.

The average total citation count in the top 100 most-cited articles was 44.4 (range 27–233) with 4.3 (range 1.9–16.6) average annual citations. Interestingly, articles in the most-cited group had on average twice the number of authors (4.82)[1–9] compared with the least-cited group (2.28)[1–8]. Single-author articles were more prevalent in the least-cited group (43) than in the most-cited group (6). Both groups comprised articles from an array of countries (Table 2). Australia produced the greatest number of articles at 47% and 47%, followed by New Zealand at 12% and 14%, in the most-cited and least-cited groups, respectively.

Perhaps unsurprisingly, original articles were well-represented in the most-cited 100 (75%), and underrepresented in the least-cited 100 (34%), compared with overall journal representation (61%). Notably, although reviews represented only 4% of journal output, 22% of the most-cited articles were reviews. In contrast, editorials and 'letters to the editor' represented a significant proportion of

Competing/conflicts of interest: No stated conflict of interest
Funding sources: No stated funding sources

Biochemical and Biophysical Research Communications 451 (2014) 510–515

Contents lists available at ScienceDirect

Biochemical and Biophysical Research Communications

journal homepage: www.elsevier.com/locate/ybbrc

The role of calpain in an *in vivo* model of oxidative stress-induced retinal ganglion cell damage

Yu Yokoyama [a], Kazuichi Maruyama [a], Kotaro Yamamoto [a], Kazuko Omodaka [a], Masayuki Yasuda [a], Noriko Himori [a], Morin Ryu [a], Koji M. Nishiguchi [a], Toru Nakazawa [a,b,c,*]

[a] Department of Ophthalmology, Tohoku University Graduate School of Medicine, Miyagi, Japan
[b] Department of Retinal Disease Control, Tohoku University Graduate School of Medicine, Miyagi, Japan
[c] Department of Advanced Ophthalmic Medicine, Tohoku University Graduate School of Medicine, Miyagi, Japan

ARTICLE INFO

Article history:
Received 29 July 2014
Available online 8 August 2014

Keywords:
Retinal ganglion cell
Oxidative stress
Apoptosis
Calpain
AAPH
SNJ-1945

ABSTRACT

Purpose: In this study, we set out to establish an *in vivo* animal model of oxidative stress in the retinal ganglion cells (RGCs) and determine whether there is a link between oxidative stress in the RGCs and the activation of calpain, a major part of the apoptotic pathway.

Materials and methods: Oxidative stress was induced in the RGCs of C57BL/6 mice by the intravitreal administration of 2,2′-azobis (2-amidinopropane) dihydrochloride (AAPH, 30 mM, 2 μl). Control eyes were injected with 2 μl of vehicle. Surviving Fluorogold (FG)-labeled RGCs were then counted in retinal flat mounts. Double staining with CellROX and Annexin V was performed to investigate the co-localization of free radical generation and apoptosis. An immunoblot assay was used both to indirectly evaluate calpain activation in the AAPH-treated eyes by confirming α-fodrin cleavage, and also to evaluate the effect of SNJ-1945 (a specific calpain inhibitor: 4% w/v, 100 mg/kg, intraperitoneal administration) in these eyes.

Results: Intravitreal administration of AAPH led to a significant decrease in FG-labeled RGCs 7 days after treatment (control: 3806.7 ± 575.2 RGCs/mm^2, AAPH: 3156.1 ± 371.2 RGCs/mm^2, $P < 0.01$). CellROX and Annexin V signals were co-localized in the FG-labeled RGCs 24 h after AAPH injection. An immunoblot assay revealed a cleaved α-fodrin band that increased significantly 24 h after AAPH administration. Intraperitoneally administered SNJ-1945 prevented the cleavage of α-fodrin and had a neuroprotective effect against AAPH-induced RGC death (AAPH: 3354.0 ± 226.9 RGCs/mm^2, AAPH+SNJ-1945: 3717.1 ± 614.6 RGCs/mm^2, $P < 0.01$).

Conclusion: AAPH administration was an effective model of oxidative stress in the RGCs, showing that oxidative stress directly activated the calpain pathway and induced RGC death. Furthermore, inhibition of the calpain pathway protected the RGCs after AAPH administration.

1. Introduction

Optic nerve fiber degeneration resulting in retinal ganglion cell (RGC) death, which occurs in diseases such as glaucoma, can threaten visual function and lead to blindness. Various studies have investigated possible treatments aimed at preventing this process, but the pathological mechanism of optic nerve degeneration and RGC loss is not yet well understood. Thus, viable neuroprotective strategies have not yet been found.

Many neuroprotective strategies have been considered so far. Among the most promising are those targeting oxidative stress, which is associated with aging. Oxidative stress has a role in the pathogenesis of various systemic diseases, and is known to induce neuronal cell death in neurodegenerative diseases such as Alzheimer's disease, amyotrophic lateral sclerosis, and Parkinson's disease [1–3]. Oxidative stress has also been implicated in glaucoma, and it is necessary to better understand the underlying mechanism of oxidative stress-induced dysfunction in order to more effectively treat this disease [4,5]. Recently, a number of studies demonstrated that optic nerve crush (NC), a commonly used model of the axonal injury that occurs in ocular diseases such as glaucoma, could help elucidate the cytotoxic role of oxidative

Abbreviations: RGC, retinal ganglion cell; AAPH, 2,2′-azobis (2-amidinopropane) dihydrochloride; FG, Fluorogold; NC, optic nerve crush; Ca^{2+}, calcium ion; DPBS, Dulbecco's phosphate-buffered saline; PFA, paraformaldehyde; CMC, carboxymethylcellulose; ROS, reactive oxygen species; AIF, apoptosis-inducing factor.

* Corresponding author at: Department of Ophthalmology, Tohoku University Graduate School of Medicine, 1-1, Seiryo, Aoba, Sendai, Miyagi 980-8574, Japan. Fax: +81 22 717 7298.
E-mail address: ntoru@oph.med.tohoku.ac.jp (T. Nakazawa).

http://dx.doi.org/10.1016/j.bbrc.2014.08.009
0006-291X/

stress in the process of RGC death [6,7]. In a previous study, we showed that mice deficient in Nrf2, a key transcription factor regulating the expression of anti-oxidant genes, had significantly fewer surviving Fluorogold (FG)-labeled RGCs than wild-type mice 7 days after NC. This result suggested that the regulation of oxidative stress signaling was a potential neuroprotective treatment for diseases affecting the optic nerve fiber and the RGCs.

Our previous research showed that the activation of calpain played a key role in the process of RGC death after NC [7]. Calpain is a member of the cysteine protease family that is regulated by increased intracellular calcium ion (Ca^{2+}) levels and is raised locally through calcium channels. A large Ca^{2+} influx into the cytosol leads to calpain activation and cell death in various pathological conditions [8–10]. However, although our previous studies showed that NC caused oxidative stress and calpain activation in the retina *in vivo*, NC is a model of axonal injury generally, not oxidative stress specifically, and therefore cannot serve as a method of directly evaluating the efficacy of neuroprotective strategies against oxidative stress.

Therefore, to directly explore the effect of oxidative stress on calpain activation, we established a new *in vivo* mouse model of RGC degeneration caused by oxidative stress, using the intravitreal administration of 2,2′-azobis (2-amidinopropane) dihydrochloride (AAPH) [11]. In this report, we use this model to attempt to determine whether the calpain pathway has a causative role in oxidative damage-induced RGC death, and whether inhibiting oxidative stress-induced calpain activation has potential as a neuroprotective treatment for ocular diseases involving oxidative stress.

2. Materials and methods

This study used adult (10–12-week old) male C57BL/6 mice (SLC, Shizuoka, Japan). All animals were maintained and handled in accordance with the ARVO Statement for the Use of Animals in Ophthalmic and Vision Research and the guidelines from the Declaration of Helsinki and Guiding Principles in the Care and Use of Animals. All experimental procedures described in the present study were approved by the Ethics Committee for Animal Experiments at Tohoku University Graduate School of Medicine.

2.1. Induction of oxidative stress in the retina

Intravitreal administration of AAPH was performed as previously described [12–14]. Briefly, each animal was anesthetized with pentobarbital (50 mg/kg). Two microliters of AAPH (30 mM) was injected intravitreally using a Hamilton syringe with a 32 G needle under surgical stereomicroscopy. The same volume of Dulbecco's phosphate-buffered saline (DPBS) was injected in the control group. If lens injuries or vitreous hemorrhaging were observed after the injection, the animals were excluded from the study.

2.2. Retrograde labeling of the RGCs and cell counting

Retrograde labeling was performed as described previously using a fluorescent tracer, FG (Fluorochrome, LLC, Denver, CO, USA), 7 days before the intravitreal injection of AAPH or DPBS [12]. Briefly, the mice were anesthetized with a mixture of ketamine (100 mg/kg) and xylazine (9 mg/kg) prepared at room temperature. Under full anesthesia, two small holes were drilled into the skull at sites corresponding to the superior colliculi, and 2 μl of 2% FG with 1% dimethylsulfoxide were injected using a Hamilton syringe with a 32 G needle. Seven days after the intravitreal injection of AAPH or DPBS, the retinas were harvested and fixed with 4% paraformaldehyde (PFA) for three hours. The retinas were then placed on glass slides with the ganglion cell layer facing up. Vectashield mounting medium (Vector Laboratories) and a cover glass were also applied. RGC survival was determined by counting FG-labeled RGCs in 12 distinct areas under the microscope [12]. Our investigation of the effect of calpain used the calpain inhibitor SNJ-1945 (Senju Pharmaceutical Co., Ltd). One day before administration of AAPH, the FG-labeled mice received an intraperitoneal administration of 4% w/v SNJ-1945 (100 mg/kg) in carboxymethylcellulose (CMC). The control group received CMC without SNJ-1945. Administration of SNJ-1945 continued daily until 7 days after the AAPH injection, when the retinas were harvested. Fixation of the retinas and RGC counting were then performed as described above.

2.3. Immunoblot assay

Immunoblotting was performed as previously described with minor modifications [13,14]. Isolated retinas were obtained surgically 3, 6 and 24 h after the intravitreal injection of AAPH or DPBS and placed in a lysis buffer (25 mM Tris–HCl; pH 7.6, 150 mM NaCl, 1% NP-40, 1% sodium deoxycholate, 0.1% SDS, 1% protease inhibitor cocktail; Sigma–Aldrich, 1% phosphatase inhibitor cocktail 2; Sigma–Aldrich). Each sample was separated with SDS–PAGE and electroblotted to polyvinylidene fluoride membranes (Immobilon-P, Millipore). After blocking the membrane with 4% BlockAce, (Yukijirushi), they were incubated with primary mouse monoclonal antibodies against α-fodrin (1:750, Abcam), and β-actin (1:5000, Sigma–Aldrich) overnight at 4 °C. The membranes were then incubated with a horseradish peroxidase-conjugated goat immunoglobulin secondary antibody. Detection of the antigen–antibody complex was performed with the ECL Prime Western Blotting Detection System (GE Healthcare). Signals were measured in Image Lab statistical software (Bio-Rad, Hercules, CA, USA) and normalized to β-actin.

2.4. Detection of free radicals and RGC apoptosis

Staining with CellROX Green Reagent (Life Technologies) and an Annexin V-Cy3 detection kit (PromoKine) were used to evaluate the generation of oxidative stress and apoptosis. One week after FG labeling, 2 μl of AAPH 30 mM was injected in the mice intravitreally. Twenty-two hours later, 1 μl of 100 μM CellROX and 25×10^{-3} μg of Annexin V-Cy3 were injected intravitreally under general anesthesia (performed with ketamine and xylazine).

The retinas were harvested 24 h after the injection of AAPH, fixed with 4% PFA for 2 h and flat-mounted. The fluorescence of the reagents was evaluated with a confocal laser microscope (LSM780, Carl Zeiss, Oberkochen, Germany).

2.5. Detection of AAPH-induced calpain activation in the RGCs

To investigate the localization of calpain activation, we stained the retinas with a fluorogenic substrate [15]. To identify the RGCs, retrograde labeling was performed as described above, with DiI (CellTracker CM-DiI, Life Technologies). One week after retrograde labeling, the left eye of each mouse received an intravitreal injection of 2 μl of 30 mM AAPH, under anesthesia. As a control, the contralateral eye was injected with 2 μl DPBS. Twenty-one hours later, both eyes received intravitreal injections of fluorogenic cell-permeable calpain substrate ((DABCYL)-TPLK~SPPPSPRE (EDANS)-RRRRRRR-NH_2 calpain substrate IV, Millipore). The retinas were harvested 24 h after AAPH injection, immediately fixed with 4% PFA for 2 h and flat mounted. The fluorescence of the fluorogenic substrate, representing the activation of calpain, was evaluated with an Axiovert 200 microscope (Carl Zeiss, Oberkochen, Germany).

2.6. Statistical analysis

Statistical analysis was performed using JMP pro 10.02 (SAS Institute Inc.) software for Windows. Continuous variables were expressed as mean values ± standard deviation. The *t*-test was used to analyze differences between pairs of groups. Multiple comparisons were done using ANOVA with Dunnett's post hoc analysis. The level of significance was 0.05 in all statistical tests.

3. Results

3.1. The effect of AAPH treatment on RGC survival

To investigate the effect of AAPH-induced oxidative stress on RGC survival, we performed the intravitreal injection of AAPH (30 mM, 2 μl) or DPBS (2 μl) in the mice. Seven days after the administration of AAPH, we counted the number of FG-labeled RGCs and found that they had significantly decreased (control: 3806.7 ± 575.2 RGCs/mm^2, AAPH: 3156.1 ± 371.2 RGCs/mm^2, $P < 0.01$, $n = 8$, Fig. 1). This finding indicated that the administration of AAPH could induce significant RGC death.

3.2. Detecting oxidative stress, calpain activation and apoptosis in the RGCs after AAPH treatment

In the control group, CellROX and Annexin V signals in the retina were not co-localized. However, in the AAPH-treated group, CellROX and Annexin V signals were co-localized with the FG-labeled RGCs 24 h after AAPH injection (Fig. 2A). This result indicated that oxidative stress occurred in the RGCs after AAPH treatment. Next, in order to confirm the activation of calpain in the RGCs, we used a fluorogenic calpain substrate to visualize calpain activation (Fig. 2B). The expression of the fluorogenic calpain substrate was co-localized with the DiI signal. This result indicated that calpain activation occurred in the RGCs 24 h after the administration of AAPH. In the control eyes, by contrast, we did not observe calpain activation in the RGCs.

3.3. Blocking calpain activation prevents RGC death caused by oxidative stress

To investigate the relationship between calpain activation and AAPH treatment, we performed a immunoblot analysis. This analysis showed that the band of cleaved α-fodrin, a substrate of calpain, was significantly detectible 24 h after AAPH administration, but not after 3 or 6 h (Fig. 3A). The intensity of the band increased significantly, by more than twofold. It is known that activated calpain can cleave α-fodrin to a size of 145 kDa. This result indicated that AAPH was able to induce RGC death through oxidative stress, and suggested that it could be related to calpain activation. We confirmed this result by treating the AAPH-injected eyes with SNJ-1945, a specific calpain inhibitor (Fig. 3B). SNJ-1945 prevented the cleavage of α-fodrin that occurred 24 h after AAPH injection (SNJ-1945 treatment: 0.6 ± 0.3-fold change vs. no treatment, $P < 0.05$, $n = 4$).

These results showed that AAPH-induced oxidative stress in the RGCs caused calpain activation and subsequent RGC death. In order to obtain further confirmation of these results, we performed the intraperitoneal administration of SNJ-1945, and found that it significantly reduced RGC death in our animal model (AAPH: 3369.8 ± 216.0 RGCs/mm^2, AAPH+SNJ-1945: 3817.8 ± 469.6 RGCs/mm^2, $P < 0.05$, Fig. 4).

4. Discussion

In this study, we used the intravitreal administration of AAPH, a free radical generator, to establish an animal model of the oxidative stress that occurs in the RGCs in neurodegenerative diseases of the eye. We found that oxidative stress in this model was associated with calpain activation in the retina and RGC death after 7 days. Moreover, AAPH administration successfully induced oxidative stress, confirmed by the finding that CellROX and Annexin V-Cy3 signals were co-localized in FG-labeled RGCs. AAPH administration also led to the activation of calpain in the retina after 24 h, confirmed by an immunoblot analysis. Moreover, the intraperitoneal administration of SNJ-1945 had a neuroprotective effect *in vivo*, preventing the cleavage of α-fodrin and RGC death after AAPH administration. These results indicate that oxidative stress-induced RGC death is mediated in part through the calpain pathway.

Previously, AAPH has been used to induce oxidative stress in non-RGC retinal cells, such as the photoreceptors, *in vitro* [16,17]. Furthermore, it has been reported that oxidative stress can induce apoptosis of the RGCs *in vitro* [18,19]. Our previous work has also demonstrated the importance of oxidative stress, by showing that mice deficient in Nrf2, a key transcription factor regulating antioxidant genes, had significantly fewer surviving FG-labeled RGCs after NC than wild-type mice [6], and that CDDO-Im, an extremely potent Nrf2 activator, prevented NC-induced RGC death *in vivo* [20]. Therefore, we expected that oxidative stress induced by AAPH would cause equivalently significant damage to the RGCs *in vivo*. Our results confirmed these expectations, showing that AAPH administration reduced the number of RGCs by 17% after 7 days.

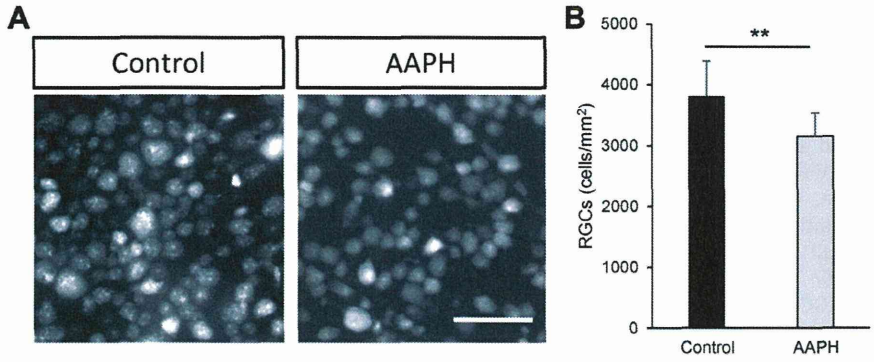

Fig. 1. Comparison of RGC density in the control and AAPH-treated groups. (A) Representative appearance of RGCs in flat-mounted retinas with quantitative data on RGC density 7 days after the intravitreal administration of AAPH. (B) Comparison of RGC density, determined by RGC counting, in the control and AAPH-treated groups. RGC density decreased significantly, by 17%, in the AAPH treatment group compared to the control group. RGC: retinal ganglion cell; scale bar: 50 μm, error bar: standard deviation; *t*-test, $^{**}P < 0.01$.